4. 代表性研究论文论著

4.1 10 篇代表性论文

nature chemistry

Article

https://doi.org/10.1038/s41557-026-02123-8

All-metal aromaticity of cyclo-Bi_3^{3-} in diuranium and dithorium inverse-sandwich-type complexes

Received: 11 July 2023

Accepted: 4 March 2026

Check for updates

Junru Ding[1], John A. Seed[2], Katrin Beuthert[3,7], Benjamin Peerless[3,7], Julia Rienmüller[3,7], Andreas Schmidt[3,7], Ashley J. Wooles[2], Louise S. Natrajan[2], Chuan-Ling Chen[4], Zhong-Ming Sun[5], Florian Weigend[6] ✉, Stefanie Dehnen[3] ✉, Jingzhen Du[1,2] ✉ & Stephen T. Liddle[2] ✉

Delocalized $[4n + 2]\pi$-aromaticity in cyclic planar unsaturated organic molecules conceptually underpins organic chemistry. Recently, the study of all-metal aromaticity has burgeoned, but although there has been interest in cyclo-$\{E_3\}$ (E = P, As, Sb, Bi) species as cyclopropenium analogues, the formation of cyclo-$\{Bi_3\}$ remains rare. Thus, the potential aromaticity of 2/6π-cyclo-$Bi_3^{\pm3-}$, as the heaviest 6*p* analogue of cyclopropylium, has remained open to different interpretations. Here we report the formation of diuranium and dithorium 6π-cyclo-Bi_3^{3-} inverse sandwich complexes, complementing the small number of acyclic- and cyclic-Bi_n ($n = 3–5$) compounds. The 6π-cyclo-Bi_3^{3-} ring exhibits substantial ring currents, similar to 6π-benzene, 2π-$(C_3H_3)^+$ or 6π-$(C_3H_3)^{3-}$. Calculations reveal similar ring currents for 6π cyclo-Bi_3^{3-}, 2π cyclo-Bi_3^{+} and 0π cyclo-Bi_3^{3+}, demonstrating σ-aromaticity that is dominant over π-aromaticity in cyclo-Bi_3^{3-}, despite the favourability of describing cyclo-Bi_3^{3-} with localized rather than delocalized bond descriptions. Confirmation of 6π-cyclo-Bi_3^{3-} σ-aromaticity provides the heaviest all-metal 6*p* analogue to π-aromatic $(C_3H_3)^{\pm3-}$, leading to organic–inorganic aromaticity benchmarking.

Q1 Delocalized Hückel $[4n + 2]\pi$-aromaticity in classical cyclic planar unsaturated organic molecules[1,2] such as benzene (C_6H_6) or the cyclopropenium cation ($(C_3H_3)^+$), which occur terrestrially and in interstellar space[3,4], conceptually underpins organic chemistry. Recently, the study of molecules exhibiting all-metal aromatic bonding[5–8] has become a burgeoning, yet intensively debated field[9–52], because whether it is appropriate to apply Hückel's model to systems beyond second-row ele-
Q2 ments remains an open question. Indeed, in the absence of consensus on the definition of aromaticity[53], discussions can only be valid within their own arbitrary criteria. Accordingly, the study of potentially aromatic all-metal species is necessary to develop further insight, and ultimately a consensus, and examples now span inorganic heterocycles with three-, four- and five-membered rings with a range of metals from lithium to thorium providing complementary or contrasting types of inorganic aromaticity to established organic aromaticity[1–52]. However, although there has been interest in cyclo-$\{E_3\}$ (E = P, As, Sb, Bi)

[1]College of Chemistry, Zhengzhou University, Zhengzhou, China. [2]Department of Chemistry and Centre for Radiochemistry Research, University of Manchester, Manchester, UK. [3]Institute of Nanotechnology, Karlsruhe Institute of Technology, Eggenstein-Leopoldshafen, Germany. [4]State Key Laboratory of Elemento-Organic Chemistry, Tianjin Key Lab for Rare Earth Materials and Applications, School of Materials Science and Engineering, Nankai University, Tianjin, China. [5]Department of Chemistry, Fudan University, Shanghai, China. [6]Institute for Quantum Materials and Technologies,

nature catalysis

Article https://doi.org/10.1038/s41929-026-01480-4

Palladium-catalysed asymmetric *anti*-Michael-type addition of α,β-unsaturated carboxylic acids with carboranes

Received: 18 November 2024

Accepted: 7 January 2026

Published online: 30 January 2026

Check for updates

Chao Lei[1,3], Wen Lu[1,3], Tingting Shen[1,3], Meng Huang[1], Yan-Xuan Wu[1], Donghui Wei[1] ✉, Yan-Na Ma[1] ✉ & Xuenian Chen[1,2] ✉

The catalytic asymmetric Michael addition of α,β-unsaturated carbonyl compounds is one of the most valuable methods for constructing the β-carbon chirality centre because of its atom economy and efficiency. However, the catalytic asymmetric reverse α-addition of a nucleophile to an α,β-unsaturated carbonyl compound is much less common. Here we realize a palladium-catalysed asymmetric α-carboranylation of α,β-unsaturated carboxylic acids via an inverse electron-demand nucleophilic addition. The reaction features good B(9)-site selectivity of *o*/*m*-carboranes, precise α-regioselectivity towards α,β-unsaturated carboxylic acids, wide functional group tolerance and excellent enantioselectivities. A detailed reaction mechanism is proposed based on experimental and computational results that elucidates the origin of the enantioselectivity and α-selectivity. This finding has a guiding significance for the catalytic asymmetric *anti*-Michael-type addition of α,β-unsaturated carbonyl compounds and provides a different avenue for synthesizing α-chiral carboxylic acids.

Icosahedral carboranes (that is, $C_2B_{10}H_{12}$), a class of representative boron clusters with three-dimensional aromaticity, have potential applications in material chemistry, organic synthesis and pharmaceuticals[1–13]. In particular, carborane derivatives are very attractive in medicinal chemistry because of their ability to form unusual dihydrogen bonds that can target hydrophobic binding sites in different bioreceptors when designing bioactive compounds[2] (Fig. 1a). In addition, carboranes are potential candidates for boron neutron capture therapy due to their high boron content[13]. Consequently, developing new methods to introduce carboranes into organic molecules is highly desirable. Over the past several decades, various cage-carbon-substituted *o*-carborane derivatives were synthesized via reactions of decaborane with alkynes or cage C−H functionalization[14,15]. However, cage-boron-substituted *o*-carborane derivatives are less known due to the weak polarity of B−H bonds and the low selectivity of ten B−H bonds in *o*/*m*-carboranes. Notably, the B-substituted carborane cage behaves as an electron-rich moiety, in contrast to the C-substituted carborane cage as electron-withdrawing, making the derivatives show different properties[16]. Therefore, the selective B−H functionalization to access cage-boron-substituted *o*-carborane derivatives is of great significance, and some pioneering work has been reported in the last decade[17–23]. Despite these, the catalytic asymmetric synthesis to connect the boron vertex with the chiral carbon centre was not reported[24–26]. Using 1,1,1,3,3,3-hexafluoro-2-propanol (HFIP) as a solvent, our group realized a series of electrophilic substitution reactions on the B(9) position of *o*-carborane[27–30] (Fig. 1b). The Pd(II)-catalysed B(9)−H functionalization has also been developed via an electrophilic palladation process[31]. In these reactions, the carborane acts as a nucleophile to react with diverse electrophiles.

Catalytic asymmetric Michael addition is one of the most valuable methods for constructing β-chirality centre of α,β-unsaturated carbonyl compounds regarding their atom economy and green credentials (Fig. 1c). Therefore, a large variety of nucleophiles (Michael donors) and α,β-unsaturated compounds (Michael acceptors) have been employed in these reactions[32–41]. By contrast, catalytic

[1]College of Chemistry, Zhengzhou University, Zhengzhou, China. [2]School of Chemistry and Chemical Engineering, Henan Key Laboratory of Boron

nature synthesis

Article

https://doi.org/10.1038/s44160-024-00607-4

Synthesis of ultrahigh-metal-density single-atom catalysts via metal sulfide-mediated atomic trapping

Received: 28 November 2023

Accepted: 14 June 2024

Published online: 15 July 2024

Check for updates

Jiangwei Chang[1], Wen Jing[1], Xue Yong[2], Ang Cao[3], Jingkun Yu[1], Han Wu[1], Chengzhang Wan[4], Siyang Wang[1], Geoffrey I. N. Waterhouse[5], Bai Yang[6], Zhiyong Tang[7], Xiangfeng Duan[4] ✉ & Siyu Lu[1] ✉

Single-atom catalysts (SACs) exhibit exceptional intrinsic activity per metal site, but are often limited by low metal loading, which compromises the overall catalytic performance. Pyrolytic strategies commonly used for synthesizing SACs generally suffer from aggregation at high metal loadings. Here we report a universal synthesis approach for ultrahigh-density metal–nitrogen–carbon (UHDM–N–C) SACs via a metal-sulfide-mediated atomization process. We show that our approach is general for transition, rare-earth and noble metals, achieving 17 SACs with metal loadings >20 wt% (including a loading of 26.9 wt% for Cu, 31.2 wt% for Dy and 33.4 wt% for Pt) at 800 °C, as well as high-entropy quinary and vicenary SACs with ultrahigh metal contents. In situ X-ray diffraction and transmission electron microscopy alongside molecular simulations reveals a dynamic nanoparticle-to-single atom transformation process, including thermally driven decomposition of the metal sulfide and the trapping of liberated metal atoms to form thermodynamically stable M–N–C moieties. Our studies indicate that a high N-doping is crucial for achieving ultrahigh-loading metal atoms and a metal-sulfide-mediated process is essential for avoiding metal aggregation at high loadings. As a demonstration, the metal-loading-dependent activity in electrocatalytic oxygen evolution reaction is demonstrated on SACs with increasing Ni content.

Since their discovery by Zhang's group[1,2], single-atom catalysts (SACs) have attracted wide interest in the field of energy-related electrocatalysis. SACs consist of atomically dispersed metals on a conductive support, typically N-doped carbon. Due to their unique geometries and electronic properties, SACs offer many advantages over traditional metal-nanoparticle-based catalysts, including (1) fully exposed active sites, (2) high atom utilization (near 100%), which is especially important for the high-cost noble metals, and (3) tunable local coordination bonds, which allow satisfactory activity and selectivity for various applications[3–6]. A wide range of methods, especially pyrolysis-based strategies, have been developed for synthesizing metal–nitrogen–carbon (M–N–C, M=Ni, Fe and so on) SACs[7–11]. However, the metal-atom loadings for most reported M–N–C SACs are typically less than 5 wt% or 1 at%, with only a few studies reporting loadings above 10 wt% (refs. 7,8,12,13). Increasing the metal loadings typically results in metal-atom aggregation and nanoparticle formation. Accordingly, the active-site density per square nanometre is typically limited to within 4 atoms nm^{-2}, which is much lower than that of commercial catalysts (for example, 20 wt% Pt/C, ~15 atoms nm^{-2}).

nature synthesis

ARTICLES

https://doi.org/10.1038/s44160-022-00114-4

Check for updates

Atroposelective isoquinolinone synthesis through cobalt-catalysed C–H activation and annulation

Xiao-Ju Si[1,2], Dandan Yang[1,2], Meng-Chan Sun[1], Donghui Wei[1], Mao-Ping Song[1] and Jun-Long Niu[1]✉

Enantioselective C–H functionalization for the synthesis of chiral molecules is a challenge in organic synthesis. Although there are several methods for atroposelective C–H functionalization to form C–N axially chiral anilides based on preformed aromatic ring systems, methods that construct N-heterocycles are relatively under-explored. Here we report a cobalt-catalysed enantioselective C–H activation and annulation process for the atroposelective synthesis of isoquinolines. The reaction proceeds under mild conditions using $Co(OAc)_2{\cdot}4H_2O$ with a chiral salicyl-oxazoline (Salox) ligand and O_2 as an oxidant. The reaction tolerates a broad range of benzamides and internal and terminal alkynes, producing a range of C–N axially chiral isoquinolinones in excellent yield and enantioselectivity (up to 98% yield and 98% e.e.). Mechanistic studies infer that the process proceeds through a Co^{III}/Co^{I} catalytic cycle, with the C–N reductive elimination step being stereo-determining. The isoquinolinone products show atropostability and thermal resistance and are suitable ligands for the Pd-catalysed enantioselective C–H functionalization of indole.

C–N axially chiral units have emerged as intriguing and promising frameworks and are widely found in natural products[1], bioactive molecules[2], privileged chiral ligands[3] and new functional materials (Fig. 1a)[4], and the synthesis of C–N atropisomers has attracted increasing attention over the past two decades. However, compared with the well-developed C–C axially chiral biaryls[5–10], the enantioselective synthesis of C–N axially chiral compounds has been explored less[11–13]. It is highly desirable to develop an efficient catalytic system that can simultaneously control both reactivity and enantioselectivity in the construction of C–N axially chiral frameworks with high atropostability.

Since the pioneering asymmetric synthesis of C–N axially chiral anilides[14,15], an array of catalytic strategies have been disclosed, including N–H functionalization[16–20], direct construction of the C–N chiral axis[21] and desymmetrization reactions[22] (Fig. 1b,(i)–(iii)). The de novo formation of an aromatic ring, based on cycloaddition, cascade annulation or the Paal–Knorr reaction, has also provided a valuable approach (Fig. 1b,(iv))[23–26]. In recent years, transition-metal-catalysed atroposelective C–H bond functionalization based on an existing aromatic ring and the C–N axis has been developed as a powerful method (Fig. 1b,(v)), with impressive progress made by other groups[27–31]. Despite these elegant works, the de novo construction of the N-heterocycle using a direct C–H activation strategy and concomitant enantiocontrol of the axial chirality is highly appealing, yet challenging.

Although enantioselective C–H functionalization is still dominated by the use of noble transition metals (Pd, Rh and Ir), recent focus has shifted to the sustainable, more abundant and less toxic 3d-metal cobalt catalyst[32–35]. In general, two strategies have been successfully applied to asymmetric cobalt catalysis: an achiral Cp^*Co^{III}/CCA (chiral carboxylic acid) system (strategy I, Fig. 1c)[36–41] and a chiral Cp^XCo^{III} system (strategy II, Fig. 1c)[42–44]. By using the first strategy, the C–H alkylation of indoles via a reversible insertion/stereo-determining protodemetalation mechanism has been carried out successfully[36]. Meanwhile, the $Cp^{*tBu}Co^{III}$/CCA-catalysed asymmetric $C(sp^3)$–H amidation of thioamides through an enantioselective $C(sp^3)$–H activation step has also been realized[37]. Another strategy was based on the use of the chiral $Cp^XCo(III)$ complex[42], as finely designed and demonstrated for asymmetric C–H alkylation[42], carboamination[43], as well as a multicomponent reaction[44]. In stark contrast to the high-valent Cp^*Co^{III}-catalysed system, the earth-abundant and readily available cobalt-catalysed asymmetric C–H functionalization remains highly elusive due to the serious lack of tailor-made chiral ligands that not only stabilize the catalytic cobalt centre, but also precisely control enantioselectivity. More recently, the cobalt-salt-catalysed $C(sp^2)$–H olefination/asymmetric alkene functionalization via a Co(II)/CPA (chiral phosphoric acid) combined catalysis has been demonstrated[45]. It is noteworthy that it is the stereoselective aza-Michael addition to maleimide, rather than the common C–H cleavage or alkene insertion/reduction elimination, that serves as the stereo-determining step, which might consequently limit further expansion of the Co(II)/CPA system. To this end, the development of versatile chiral ligands and novel protocols with the inexpensive cobalt salt as catalyst to realize asymmetric C–H functionalization remains a daunting challenge (strategy III, Fig. 1c)[46].

Inspired by the pioneering cobalt-catalysed C–H activation/annulation reported in ref. [47], and with our continuing interest in cobalt catalysis[48], in this Article we describe cobalt-catalysed enantioselective C–H activation/annulation assisted by a precisely designed Salox chiral ligand, affording a type of C–N axially chiral compound containing isoquinolinone frameworks (Fig. 1d). Notable features of this protocol include (1) the cobalt-salt-enabled C–N chiral axis construction, (2) easily prepared chiral ligands (one step), (3) environmentally friendly O_2 as an oxidant, (4) the broad substrate scope, high yields and excellent enantioselectivities and (5) its unique atropostability, with a high barrier to rotation for the C–N axially chiral product.

Results

Optimization of the reaction conditions. Initially, we investigated the annulation reaction between benzamide (**1a**) and diphenylacetylene (**2a**) for the atroposelective synthesis of isoquinolinone

Signal Transduction and Targeted Therapy www.nature.com/sigtrans

REVIEW ARTICLE OPEN

Targeting epigenetic regulators to overcome drug resistance in cancers

Nan Wang[1], Ting Ma[1]✉ and Bin Yu[1]✉

Drug resistance is mainly responsible for cancer recurrence and poor prognosis. Epigenetic regulation is a heritable change in gene expressions independent of nucleotide sequence changes. As the common epigenetic regulation mechanisms, DNA methylation, histone modification, and non-coding RNA regulation have been well studied. Increasing evidence has shown that aberrant epigenetic regulations contribute to tumor resistance. Therefore, targeting epigenetic regulators represents an effective strategy to reverse drug resistance. In this review, we mainly summarize the roles of epigenetic regulation in tumor resistance. In addition, as the essential factors for epigenetic modifications, histone demethylases mediate the histone or genomic DNA modifications. Herein, we comprehensively describe the functions of the histone demethylase family including the lysine-specific demethylase family, the Jumonji C-domain-containing demethylase family, and the histone arginine demethylase family, and fully discuss their regulatory mechanisms related to cancer drug resistance. In addition, therapeutic strategies, including small-molecule inhibitors and small interfering RNA targeting histone demethylases to overcome drug resistance, are also described.

Signal Transduction and Targeted Therapy (2023)8:69 ; https://doi.org/10.1038/s41392-023-01341-7

INTRODUCTION

Increasing evidence has suggested that the incidence of multiple cancers has been rising year by year in the world.[1] Although great progress has been made in the treatment of cancer, it is still the main cause of death. Chemotherapy, radiotherapy, immunotherapy, surgical resection, and targeted cancer therapies are usually used in cancer treatment.[2–5] Generally, good therapeutic effects can be achieved in the early stage of cancer, but after long-term treatment with chemotherapeutic drugs, tumor cells could develop drug resistance. Drug resistance is closely related to poor prognosis and cancer recurrence, which is one of the main reasons for cancer treatment failure. Therefore, it is desirable to elucidate the resistance mechanisms in tumor cells during treatment.

To date, there are many identified drug resistance mechanisms (Fig. 1). As a member of ATP-binding cassette (ABC) transporters, P-glycoprotein (P-gp) can promote the efflux of drugs and make the drugs lose their therapeutic effect, inhibition of P-gp can significantly reverse drug resistance.[6–10] Additionally, cytoprotective autophagic response often counteracts apoptosis triggered by anticancer drugs, potentially contributing to acquired drug resistance.[11,12] Notably, it is generally believed that eliminating cancer stem cells (CSCs) and reversing epithelial-mesenchymal transition (EMT) are also effective means to overcome drug resistance.[13–16] Additionally, gene mutations also contribute to drug resistance, especially the resistance to tyrosine kinase inhibitors. EGFR mutation can usually lead to resistance to tyrosine kinase inhibitors, and Bruton's tyrosine kinase mutation can also result in resistance to ibrutinib.[17–19]

In addition to these factors mentioned above, epigenetic regulation is also important in mediating drug resistance (Fig. 2). Epigenetic modifications refer to the heritable changes in gene expression without changes in DNA sequence, including DNA methylation, histone modification, X-chromatin remodeling, non-coding RNA, nucleosome localization and genomic imprinting.[20,21] Of note, modifications of DNA and histone not only affect the function of transcription factors, but also tightly associate with other epigenetic modifications such as chromatin remodeling and non-coding RNAs to co-regulate neoplastic processes.[22,23] Generally, DNA methylation often affects gene expression, transcription, and activity. Under the action of DNA methyltransferase, a methyl group is covalently added to the C-5 position of the DNA cytosine ring, and hypermethylation of gene promoters usually leads to transcriptional inhibition, resulting in decreased gene expression.[24–26]

Similarly, covalent histone modification is also an important epigenetic model, which includes acetylation, phosphorylation, methylation, ADP ribosylation, ubiquitination, and citrullination, etc.[27–31] Among these modifications, most of the studies have focused on the acetylation, methylation, and phosphorylation. Numerous studies have shown that covalent post-translational modification of histone tails is critical to the occurrence and development of cancer, including histone demethylases, histone methyltransferases, histone deacetylases, histone acetyltransferases (HATs), and ADP ribosyltransferases.[32–35] For example, it has been shown that histone acetylation is closely associated with gene transcription and the alterations of histone acetylation are tightly associated with cancer phenotypes in multiple cancers.[36,37] Furthermore, cancer cells can produce significant resistance to chemotherapeutic drugs through epigenetic changes, especially abnormal modification of histone or genomic DNA.[38,39] Their dysregulation usually results in the activation of oncogenes or the inactivation of tumor suppressor genes as well as the dysfunction of many signaling pathways. Therefore, targeting epigenetic modifications could be a promising strategy to overcome drug

[1]Institute of Drug Discovery & Development, School of Pharmaceutical Sciences, Zhengzhou University, Zhengzhou 450001, China
Correspondence: Ting Ma (mating@zzu.edu.cn) or Bin Yu (yubin@zzu.edu.cn)

Received: 21 August 2022 Revised: 15 January 2023 Accepted: 28 January 2023

Signal Transduction and Targeted Therapy www.nature.com/sigtrans

RESEARCH HIGHLIGHT OPEN

Azvudine (FNC): a promising clinical candidate for COVID-19 treatment

Bin Yu[1] and Junbiao Chang[1,2]

Signal Transduction and Targeted Therapy (2020)5:236 ; https://doi.org/10.1038/s41392-020-00351-z

A very recent work published in *Advanced Science* by our group reveals that 2′-deoxy-2′-β-fluoro-4′-azidocytidine (Azvudine, FNC), a clinical candidate originally developed for HIV treatment, has entered clinical trial in China for evaluating its efficacy and safety (ChiCTR2000029853), showing promise for treating novel coronavirus disease 2019 (COVID-19).[1] This work suggests that nucleoside-based antivirus agents could be repurposed for COVID-19 treatment.

Since the breakout of severe acute respiratory syndrome coronavirus 2 (SARS-COV-2) in December 2019, SARS-COV-2 has spread rapidly. As of August 30, 2020, over 23 million cases have been confirmed worldwide, and more than 0.8 million deaths have been reported. Because of the lack of effective treatment, the fetal cases are increasing globally, particularly in the USA. Therefore, the development of effective vaccines and drugs have been highly pursued for COVID-19 prevention and treatment. To date, some drugs and clinical drug candidates are currently undergoing clinical assessment for treating COVID-19.[2] Remdesivir, originally developed by Gilead Sciences for treating Ebola virus disease, shows effectiveness in inhibiting the activity of SARS-COV-2 and has received approval in some countries for emergency use in patients with severe COVID-19.[3] However, rationed supply, side effects, and unsatisfactory phase III clinical results limit the clinical use of remdesivir. In addition, the increasing SARS-COV-2 mutated strains G, GH and GR have posed new challenges for COVID-19 treatment.[4] Thus, it is urgent to develop safe and effective drugs for treating COVID-19.

SARS-COV-2, a positive-sense single-stranded RNA virus, utilizes nucleosides and nucleotides for RNA synthesis (Fig. 1a). Inside the host cells, nucleoside analogs mimic natural nucleosides and are transformed into corresponding active nucleoside triphosphates through kinase catalysis, which are then embedded in virus RNA during RNA synthesis and then block addition of nucleotides to the 3′-hydroxy group, finally terminating RNA chain synthesis and virus replication (Fig. 1b). Besides, nucleoside-based antiviral agents also inhibit DNA- and RNA-dependent polymerases crucial for viral replication. Therefore, the widely used nucleoside-based antiviral drugs in clinic may have potential for COVID-19 treatment.

FNC, a novel nucleoside-based broad-spectrum anti-virus clinical candidate recently developed in our laboratory for HIV infection treatment and prevention,[5] is the first dual-targeting nucleoside-based agent that inhibits nucleoside reverse transcriptase and restores expression of cytidine deaminase APOBEC3G (A3G) in HIV-1 patients derived $CD4^{+}$ T cells. The 2′-fluoro group enhances its acidic stability and greatly affects the electronic properties and conformational shape of nucleosides, thus dramatically improving the activities, while modifications at the 4′-position such as introduction of an azido group make the nucleosides adopt an unnatural 3′-C-*endo* conformation, making the compounds being active against HIV and multidrug-resistant HIV strains. FNC has exhibited desirable pharmacokinetics, excellent efficacy and safety in the phase I and II clinical trials (GQ-FNC-2014-2, GQ-FNC-201, and NCT04109183) for treating HIV infection. On March 17, 2020, a phase III clinical trial of FNC was initiated to evaluate the efficacy and safety in HIV-infected treatment naive patients (NCT04303598). On August 12, 2020, the listing application of FNC for HIV treatment was given priority in the review process (CXHS2000016/CXHS2000017). Based on our previous findings, we speculate that FNC could be repurposed for COVID-19 treatment, even for patients infected by mutated SARS-COV-2.

To evaluate the efficacy and safety of FNC in patients with mild and common COVID-19, we recently conducted a randomized, open-label, controlled clinical trial of FNC tablets in China (ChiCTR2000029853).[1] In this pilot study, 20 patients were randomly assigned to receive FNC or standard antiviral treatment. We found that FNC could shorten the nucleic acid negative conversion (NANC) time. In the FNC group, the mean times of the first NANC is 2.60 d, while for the control group, this value is 5.60 d. The NANC rate is 100% after treatment for 4 d in the FNC group, significantly higher than that (73% after 28 d treatment) in the hydroxychloroquine treatment group. FNC is also efficacious in patients who have received other treatment regimens and could help patients recover faster. Besides, FNC is well tolerated without drug-related adverse events in the FNC group. We speculate that FNC triphosphate could be embedded during RNA synthesis of SARS-COV-2 and inhibits related polymerases, finally leading to RNA replication termination (Fig. 1c). Overall, FNC is a safe and efficacious nucleoside-based drug candidate for treating mild and common COVID-19 and also shows promise for curing severe COVID-19, clinical trials with larger sample size are warranted to further investigate the efficacy and safety of FNC for COVID-19 treatment. The data also suggest that repurposing existing broad-spectrum antivirus agents is a viable and promising strategy for COVID-19 treatment.

[1]School of Pharmaceutical Sciences, Zhengzhou University, 450001 Zhengzhou, China and [2]Henan Key Laboratory of Organic Functional Molecule and Drug Innovation, College of Life Science and College of Chemistry and Chemical Engineering, Henan Normal University, 453007 Xinxiang, China
Correspondence: Junbiao Chang (changjunbiao@zzu.edu.cn)

Received: 2 September 2020 Revised: 11 September 2020 Accepted: 23 September 2020

JOURNAL OF THE AMERICAN CHEMICAL SOCIETY

pubs.acs.org/JACS

Article

Ultrastable Copper Cluster Enables Highly Site-Selective and Chemoselective Carbocation $C(sp^3)-H$ and $C(sp^2)-H$ Bonds Functionalization

Teng Jia, Cai-Fang Sun, Miao-Miao Zhang, Jie Ai, Yi-Xin Li, Zheng Wang, Yu Lan, Xin-Qi Hao,* and Shuang-Quan Zang*

Cite This: J. Am. Chem. Soc. 2025, 147, 35128–35138

Read Online

ACCESS | Metrics & More | Article Recommendations | Supporting Information

ABSTRACT: The C–H functionalization represents a universal and important method for constructing new C–C bonds by carrying out reactions directly on inert C–H bonds. The major challenges are to control the site-selectivity and chemoselectivity because most complex organic compounds have many similar C–H bonds or different functional groups, such as a C=C bond or O–H bond. Here, we develop a versatile copper cluster ($Cu_3NC^{(NHC)}$) with high stability and dynamic catalytic sites. Unlike traditional copper catalysts (which activate diazoesters to form intermediate Cu-carbenes, catalyzing cyclopropanation and O–H insertion), the $Cu_3NC^{(NHC)}$, as a versatile catalyst, has resolved the site-selective and chemoselective challenges of the $C(sp^3)-H$ bond and $C(sp^2)-H$ bond functionalization by forming $Cu_3NC^{(NHC)}$ stabilized carbocations. Moreover, turnover number (TON) values of the C–H functionalization are elevated to a whole new level (up to 123,200). Mechanistic studies and density functional theory (DFT) demonstrate that site-selectivity and chemoselectivity derive from the energy differences among these key intermediates. The diverse applicability of $Cu_3NC^{(NHC)}$ provides a generic platform for optimizing chemical reactions and fostering their innovative development, thereby promoting the rapid development of the intersection between cluster chemistry and organic chemistry.

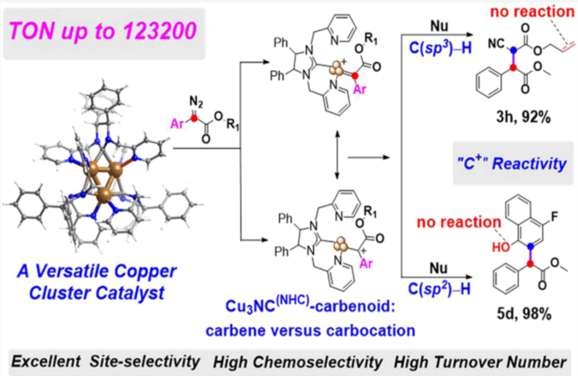

■ INTRODUCTION

The C–H functionalization has enhanced chemical synthesis by affording a streamlined method for constructing C–C bonds, which is the most important organic transformation in organic chemistry, materials science, and the synthesis of pharmaceuticals.[1−7] The development of innovative catalysts has greatly promoted the substantial progress of the above organic reactions, enhancing their utility and tolerability.[8] However, there are still many challenges in this process. The $C(sp^3)-H$ bonds are far less reactive and more difficult to functionalize selectively. Site-selectivity is a major challenge in the $C(sp^3)-H$ bonds and $C(sp^2)-H$ bonds functionalization (Scheme 1a,1b). The developed strategy relied on substrate control, such as a directing group (DG)[9,10] and a more reactive C–H bond,[11] to resolve the site-selectivity problem. The structure of the substrate may limit the applications of these approaches. A more challenging method is to use catalysts to control site-selectivity.[12,13] Meanwhile, chemoselectivity is another important challenge in C–H functionalization (Scheme 1b). Most of the reported transition metal catalysts were used to catalyze the addition reactions of α-diazoesters according to the typical carbene reactivity, thus realizing selective nucleophilic addition

provide cyclopropane compounds or O–H functionalization products.[14−20] It is also a challenging task to achieve a chemoselective electrophilic substitution on diazoesters through the reasonable and novel design of a catalyst. In addition, the turnover number (TON) of these transformations is usually less than several hundred, and improving catalytic activity is also a challenge.[17−20] Another urgent issue that needs to be addressed is the lack of multifunctional catalysts to solve comprehensively the above problems. A versatile catalyst with diverse reactivity is highly desirable.

Ligand-protected metal nanoclusters (NCs) have been rapidly developed in organic catalysis and electrochemical catalysis as representative nanocatalysts because of good chemical purity, homogeneous distribution of catalytic sites, and well-defined crystal structure.[21−25] Moreover, metal nano-

Received: July 29, 2025
Revised: August 26, 2025
Accepted: August 27, 2025
Published: September 10, 2025

JACS
JOURNAL OF THE AMERICAN CHEMICAL SOCIETY

pubs.acs.org/JACS

Article

Tailoring Methane Oxidative Coupling Pathways through Cluster-Modified Photocatalysts

Hui-Ling Luo, Hui-Li Chai, Fang-Yu Cao, Jin-Meng Cai, Jing-Zheng Zhang,* Zhao-Yang Wang,* and Shuang-Quan Zang*

Cite This: *J. Am. Chem. Soc.* 2026, 148, 9860−9869

Read Online

ACCESS | Metrics & More | Article Recommendations | Supporting Information

ABSTRACT: Photocatalytic methane coupling represents a promising strategy for the production of valuable C_{2+} chemicals. Herein, the rational design of an $Au_{24}Zn_1$ nanocluster-embedded ZnO catalyst was demonstrated to enhance photocatalytic performance, and the resultant $Au_{24}Zn_1$/ZnO catalyst exhibited a C_{2+} selectivity of 93.5% and a yield of 663.1 μmol·g_{cat}^{-1}·h^{-1} (510.1 mmol·g_{Au}^{-1}·h^{-1}) in a batch reactor. X-ray photoelectron spectroscopy (XPS) and diffuse reflectance infrared Fourier transform spectroscopy−CO adsorption (CO−DRIFTS) revealed that the clusters functioned as hole acceptors, thereby accelerating the separation of photogenerated carriers. Radical experiments and isotope-labeling studies confirmed that the •OH radical derived from water serves as the primary reactive oxygen species responsible for activating methane to •CH_3 radicals under the coexistence of H_2O and O_2, which demonstrates a significant discrepancy compared to the reported photogenerated hole activation pathway. Additionally, the •OOH radical generated via oxygen reduction played a supporting role both in modulating the concentration of •OH radicals and promoting the catalytic cycle. The cooperation contributed to the high yield and excellent selectivity of the C_{2+} products. This work provides valuable insights into the mechanistic pathway of methane conversion and highlights the potential of metal nanocluster-based materials in photocatalysis.

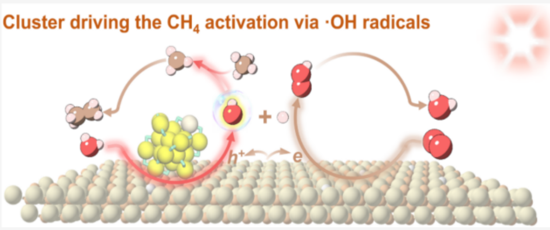

1. INTRODUCTION

As the second-largest greenhouse gas in the world, methane has a global warming potential of 81.2 times that of carbon dioxide over a 20-year time horizon.[1] Furthermore, methane functions not merely as an eco-friendly fuel source but also as a foundational molecular platform for synthesizing high-value chemical compounds.[2−4] This dual utility underscores the multifaceted advantages of methane utilization in terms of the economy, society, and security. Nevertheless, methane activation remains inherently challenging owing to its symmetrical tetrahedral configuration, minimal polarizability, and high C−H bond energy, thereby requiring extreme operational parameters, including elevated temperatures, high-pressure environments, and aggressive oxidizing agents.[5,6] The introduction of photocatalysis has markedly reduced the energy barrier, enabling the activation of C−H bonds in methane under mild conditions. This development positions methane conversion as an alternative and promising approach to address the methane surplus issues.[4,7−11] As an emerging field, photocatalytic methane conversion has attracted considerable attention in recent years, with the production of various value-added chemicals,[12] including oxygenated compounds,[13−16] such as methanol,[17−21] formic acid,[22,23] and acetic acid,[24,25] as well as alkanes such as ethane[26−33] and ethylene.[34−36]

The photocatalytic coupling of methane is an economically

C_{2+} chemicals. Typically, oxidative coupling of methane (OCM) is thermodynamically favorable ($G^0_{298\ K}$ = −320 kJ·mol^{-1}),[7,37] allowing for high yields but also leading to overoxidation products. In contrast, nonoxidative coupling of methane (NOCM) is endothermic ($G^0_{298\ K}$ = +68.6 kJ·mol^{-1}),[9] resulting in undesired activity but ideal selectivity due to the absence of excessive oxidation. Therefore, the simultaneous achievement of high activity and high selectivity in the photocatalytic coupling of methane has long been a fascinating but challenging target, especially under batch reactor conditions. Studies have shown that modulating the active species involved in the direct oxidation of methane can significantly enhance catalytic performance.[28,38] Ideally, these active species should exhibit adequate oxidative capacity, optimal concentration, and appropriate characteristics.[28,38] Excessively strong oxidative capacity or high concentrations can cause overoxidation,[10,16,39] while an abundance of active species can lead to product diversity,[40,41] both of which diminish selectivity. Conversely, insufficient oxidative capacity or low concentrations compromise catalytic activity.[11] There-

Received: December 10, 2025
Revised: February 3, 2026
Accepted: February 18, 2026
Published: February 23, 2026

JACS
JOURNAL OF THE AMERICAN CHEMICAL SOCIETY
pubs.acs.org/JACS
Article

Atomic-Precise Active Site Surgery on Carboranylthiolate-Protected Silver Nanocluster Catalysts

Jia-Hong Huang, Han Zhang, Zhao-Yang Wang,* Jia-Hua Hu, Jing Li, Jinmeng Cai,* and Shuang-Quan Zang*

Cite This: J. Am. Chem. Soc. 2025, 147, 16593−16601

ABSTRACT: Although significant progress has been made in precisely modulating the composition and structure of metal nanoclusters to tailor their properties, the well-controlled synthesis of metal nanoclusters with unsaturated coordination environments and highly active sites to enhance the catalytic performance remains remarkably challenging. Here, we propose an atomic-level surgical strategy involving the stepwise creation and manipulation of active metal sites on metal nanoclusters. A newly constructed **$Ag_{17}P$** nanocluster, costabilized by carboranethiolate and phosphine ligands, features an Ag_{13} icosahedral kernel capped by four tetrahedrally symmetrical silver atoms. Taking advantage of the phosphine ligands readily dissociating from the four peripheral silver atoms under solvent regulation, **$Ag_{17}P$** could transform into **Ag_{17}** with four exposed silver atoms. Furthermore, site-specific substitution could be accomplished in these open metal sites through a judicious choice of heterometal, resulting in an isostructural Cu-doping **$Ag_{13}Cu_4$** nanocluster. As a result, **Ag_{17}** and **$Ag_{13}Cu_4$** with exposed metal sites showed improved catalytic activities in electrocatalytic nitrate reduction reaction (NO_3RR) compared to **$Ag_{17}P$**, and **$Ag_{13}Cu_4$** displayed superior performance with an optimal faradaic efficiency (FE) of 90.4 ± 0.2% for NH_3 production and a total FE of 99.6 ± 0.3%. This study not only offers a pathway for generating and manipulating open metal sites on metal nanoclusters but also provides new perspectives for the design and synthesis of efficient metal nanocluster-based catalytic materials.

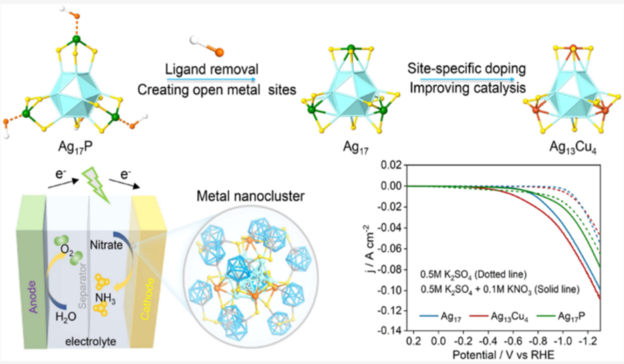

■ INTRODUCTION

As an emerging class of nanomaterials, atomically precise metal nanoclusters feature with quantum confinement effect, thus giving rise to unique electronic configurations and potential applications.[1−8] Recently, metal nanoclusters have attracted remarkable attention as model nanocatalysts owing to their atomic precision, enabling the atomic-level elucidation of the catalytic processes.[9,10] Surface and interface coordination structures have been demonstrated to determine the catalytic active sites of metal nanoclusters.[11,12] Thus, surface engineering strategies are being developed to regulate the surface environments of metal nanoclusters.[13] However, the precise creation and further directional manipulation of accessible metal sites for improving the catalytic activity and selectivity remain challenging.

Creating uncoordinated metal sites by ligand removal while preserving the inherent structural integrity continues to be a persistent pursuit for metal nanocluster catalysts.[14,15] However, ligand removal is typically achieved under harsh pretreatment (thermal and chemical methods) or in situ catalytic processes,[16−20] resulting in derivatives with distinct structural changes, size enlargement, and complicated intermediates, relationships (Scheme 1a). Auxiliary phosphine ligands have been widely utilized in costabilizing metal nanoclusters because of their monocoordination mode, which differs from traditional thiolate and alkyne-based ligands and effectively complements the vacant coordination sites.[21−24] The intrinsic neutrality of phosphine ligands and weaker M−P bonding suggest that ligand removal could occur under relatively mild conditions. Electrospray ionization mass spectrometry (ESI-MS) also confirms that the phosphine ligands are easily dissociated during the ionization process and the derived gas-phase metal nanoclusters could keep their major components.[25−27] However, the precise phosphine dissociation process involving structure evolution hitherto remains unobserved.

Following the creation, the precise manipulation of metal active sites is also conducive to improving the surface activity of metal nanoclusters. Heterometal doping has proven to be an

Received: March 10, 2025
Revised: April 22, 2025
Accepted: April 25, 2025
Published: April 30, 2025

J|A|C|S
JOURNAL OF THE AMERICAN CHEMICAL SOCIETY
pubs.acs.org/JACS Article

Thiacalix[4]arene Etching of an Anisotropic $Cu_{70}H_{22}$ Intermediate for Accessing Robust Modularly Assembled Copper Nanoclusters

Hao-Nan Qin, Meng-Wei He, Jie Wang, Hai-Yang Li,* Zhao-Yang Wang,* Shuang-Quan Zang,* and Thomas C. W. Mak

Cite This: J. Am. Chem. Soc. 2024, 146, 3545−3552 Read Online

ACCESS | Metrics & More | Article Recommendations | Supporting Information

ABSTRACT: Atom-precise metal nanoclusters (NCs) with large bulk (nuclearity >60) are important species for insight into the embryonic phase of metal nanoparticles and their top-down etching synthesis. Herein, we report a metastable rod-shaped 70-nuclei copper-hydride NC, $[Cl@Cu_{70}H_{22}(PhC{\equiv}C)_{29}(CF_3COO)_{16}]^{2+}$ (**Cu_{70}**), with Cl^- as the template, in which the $Cl@Cu_{59}$ kernel adopts a distinctive metal packing mode along the bipolar direction, and the protective ligand shell exhibits corresponding site differentiation. In terms of metal nuclearity, **Cu_{70}** is the largest alkynyl-stabilized Cu-hydride cluster to date. As a typical highly active intermediate, **Cu_{70}** could undergo a transformation into a series of robust modularly assembled Cu clusters (**B**-type **Cu_8**, **A−A**-type **Cu_{22}**, **A−B**-type **Cu_{23}**, and **A−B−A**-type **Cu_{38}**) upon etching by *p-tert*-butylthiacalix[4]arene (H_4TC_4A), which could not be achieved by "one-pot" synthetic methods. Notably, the patterns of **A** and **B** blocks in the Cu NCs could be effectively modulated by employing appropriate counterions and blockers, and the modular assembly mechanism was illustrated through comprehensive solution chemistry analysis using HR-ESI-MS. Furthermore, catalytic investigations reveal that **Cu_{38}** could serve as a highly efficient catalyst for the cycloaddition of propargylic amines with CO_2 under mild conditions. This work not only enriched the family of high-nuclear copper-hydride NCs but also provided new insights into the growth mechanism of metal NCs.

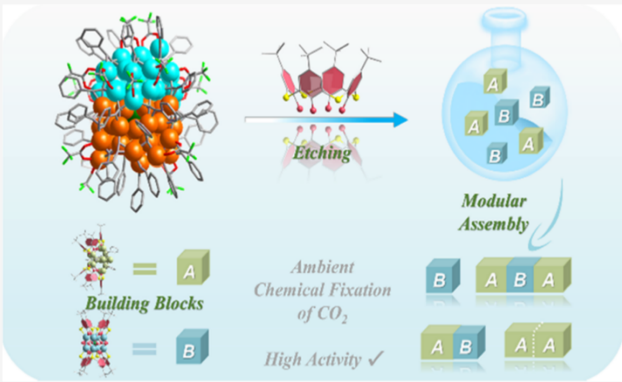

■ INTRODUCTION

Atomically precise coinage-metal nanoclusters (NCs) have attracted much attention because of their intriguing esthetic structures, unique properties, and potential applications in various research areas such as optics, catalysis, biochemistry, new energy sources, sensors, etc.[1−7] With the advancements in synthetic approaches and X-ray diffraction technology, a series of high-nuclearity Au and Ag NCs (such as Au_{99}, Au_{144}, Au_{279}, Ag_{100}, Ag_{141}, Ag_{307}) have been successfully isolated and structurally characterized, which are significant for understanding the process of formation and growth of metal nanoparticles (NPs).[8−13] In contrast, the access and precise characterization of their Cu analogs remain deficient because of the susceptibility to air oxidation and challenge in single-crystal growth, despite the pivotal role played by copper and copper-based nanomaterials in energy conversion.[14−18] Over the past decades, only limited large-sized Cu NCs (Cu_{53}, Cu_{57}, Cu_{61}, Cu_{81}, Cu_{92}, etc.) have been structurally determined, which impeded the comprehensive understanding of the evolutionary mechanisms underlying Cu nanoparticles.[19−24] Therefore, the development of new methods and approaches

The labile nanoparticle precursors and unique foreign ligands play a crucial role in cluster conversion for accessing novel metal NCs, which also provides valuable insights into the reactivity of metal clusters.[25−28] Of particular attention are metal-hydride clusters, which can serve as useful benchmark models of size evolution.[29−32] Recently, there have been several studies focusing on copper-hydride clusters that exhibit remarkable reactivity as potential precursors for expanding structural libraries or generating functional materials.[33−35] Liu et al. utilized the $Cu_{11}H_2$ clusters as templates to produce three different compounds, $Cu_{12}H_2$, $AgCu_{14}H_2$, and $AuCu_{11}$.[36] Zheng et al. introduced Pt^{4+} ions into $Cu_{32}H_8$ to obtain Pt_2Cu_{34}.[37] It is worth noting that the success of size expansion and core alloying relies on the presence of a relatively stable template, as analogous structures were consistently observed.[38,39] Alternatively, some researchers have proposed

Received: December 11, 2023
Revised: January 11, 2024
Accepted: January 16, 2024
Published: January 26, 2024

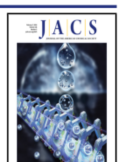

4. 代表性研究论文论著

4.2　3 部代表性论著

Drug Discovery Stories

From Bench to Bedside

Edited by
Bin Yu
Peng Zhan

Volume 2

Drug Discovery Stories

Edited by
Bin Yu
Peng Zhan

WILEY-VCH

Yu Lan

Computational Methods in Organometallic Catalysis

From Elementary Reaction to Mechanism

4. 代表性研究论文论著

4.3 其他代表性论文

	2025 年 高 水 平 论 文			
序号	**通讯作者**	**论 文 题 目**	**期 刊**	**出版时间**
1	臧双全、王朝阳	Carborane Meets Metal Nanocluster: New Opportunities in Nanomaterials	Accounts of Chemical Research	2025
2	盖军民（第一作者）	Edge Electron Effect Induced High-Entropy SEI for Durable Anode-Free Sodium Batteries	Advanced Materials	2025
3	郭玮	Regulating Interface Engineering by Helmholtz Plane Reconstructed Achieves Highly Reversible Zinc Metal Anodes	Advanced Materials	2025
4	郭玮	From Irreversible to Reversible: Nucleophilic Reactions Enhance Fast Kinetics and Superior Cycling Stability in High Voltage Lithium-Organosulfur Batteries	Advanced Materials	2025

5	李翔	Beyond Inducing Anionic Redox: Controllable Migration Sequence of Li Ions in Transition Metal Layers toward Highly Stable Li-Rich Cathodes	Advanced Materials	2025
6	卢思宇	Heteroatom-doping and conjugation-extension enable ultrahigh-bright full-color carbon quant4um dots for tunable liquid-state lasers and 3D printing	Advanced Materials	2025
7	卢思宇	Rhodamine B-Derived Low-Toxicity Full-Color Carbon Dots with Wide Tunable High-Stable Liquid-State Lasers	Advanced Materials	2025
8	卢思宇	Exploring Carbon Dots for Biological Lasers	Advanced Materials	2025
9	卢思宇	Heteroatom-Doping and Conjugation-Extension Enable Ultrahigh-Bright Full-Color Carbon Quantum Dots for Tunable Liquid-State Lasers and 3D Printing	Advanced Materials	2025
10	彭鹏	Chemical Flexibility of Atomically Precise Metal Clusters	Advanced Materials	2025
11	孙晨凯	Fine-Tuning of Molecular Self-Assembly Morphology via Synergistic Ternary Copolymerization and Side Chain Optimization of Low-Cost Polymer Donors Toward Efficient Organic Solar Cells	Advanced Materials	2025
12	臧双全、蔡金孟	Introducing La into a Customized Dual Cu Covalent Organic Framework to Steer CO2 Electroreduction Selectivity from C2H4 to CH4	Advanced Materials	2025
13	臧双全、韩振	Assembling Octahedral Pt2Ag4 Clusters for High-Efficiency Circularly Polarized Luminescence	Advanced Materials	2025

14	臧双全、李恺	Monitoring α/β Particles Using a Copper Cluster Scintillator Detector	Advanced Materials	2025
15	臧双全、王锐	Accurate Thermal Resection of Atomically Precise Copper Clusters to Achieve Near-IR Light-Driven CO2 Reduction	Advanced Materials	2025
16	张懿强	Initiating Strain Field for Mitigating Lead Leakage in Perovskite Solar Cells with Built-in Encapsulating Networks, Advanced Materials	Advanced Materials	2025
17	张懿强	Dual-Mode Molecular Regulation of Perovskite Crystallization Enables Efficient and Stable FAPbI3 Solar Cells and Modules	Advanced Materials	2025
18	赵英杰（通讯作者）	Stress Release of Single Crystal Arrays Bridged by SAM Interface Toward Highly Mechanically Durable Flexible Perovskite NIR Photodetector	Advanced Materials	2025
19	陈卫华	Superstructure Engineering Enables NASICON-Type Phosphate Cathodes with Increased Working Voltage and Energy Density	Advanced Materials	2025
20	卢思宇	Adjusting TADF and Phosphorescence for Tailored Dynamic Time-Dependent Afterglow Colored Carbon Dots spanning Full Visible Region	Angewandte Chemie International Edition	2025
21	卢思宇	Synergistic Rigidity-Enhancement and Electron-Rich Systems Engineering Robust Carbon Dots-Based Ultra-Narrowband NIR Emitters for LEDs with Superior Operational Stability	Angewandte Chemie International Edition	2025

22	卢思宇	Broadly Tunable Liquid-State Lasers and Solid-State Single-Longitudinal-Mode Near-Infrared Lasers Utilizing Halogen-Doped Graphene Quantum Dots	Angewandte Chemie International Edition	2025
23	卢思宇	CsPbBr3 Superstructures with Circularly Polarized PhotoluminesCence Obtained by the Self-Assembly and Annealing of Nanoclusters	Angewandte Chemie International Edition	2025
24	卢思宇	Visible Light Excited Time-Dependent Phosphorescence Color Tuning in Carbon Dots via Charge Transfer	Angewandte Chemie International Edition	2025
25	卢思宇	Adjusting TADF and Phosphorescence for Tailored Dynamic TimeDependent Afterglow Colored Carbon Dots spanning Full Visible Region	Angewandte Chemie International Edition	2025
26	梅光建	A Chemically Powered Rotary Molecular Motor Based on Reversible Oxazepine Formation	Angewandte Chemie International Edition	2025
27	牛林彬	Heterocoupling Two Similar Benzyl Radicals by Dual Photoredox/Cobalt Catalysis	Angewandte Chemie International Edition	2025
28	武现丽	Axial Phosphate Coordination Driven Spin State Change in FeN4 Site for Stable Oxygen Reduction	Angewandte Chemie International Edition	2025
29	杨明睿	Photogenerated Holes Induced Deep Sodium Storage of TiO2/CdSe/NFPP Cathode for High-Efficiency Photorechargeable Sodium Batteries	Angewandte Chemie International Edition	2025

30	臧双全	Au6Cu2 Clusters with High Electron Affinity and Oxygen-Mimetic Properties for Hypoxic Tumor Radiosensitization	Angewandte Chemie International Edition	2025
31	臧双全、蔡金孟	Ligand-Mediated Activity of Cu4 Clusters Boosts ElectrocatalyticNitrate Reduction	Angewandte Chemie International Edition	2025
32	臧双全、蔡金孟	Unveiling Ionized Interfacial Water-Induced Localized H* Enrichment for Electrocatalytic Nitrate Reduction	Angewandte Chemie International Edition	2025
33	臧双全、冯鹏飞	Amino-Acid-Induced Circularly Polarized Luminescence of Octahedral Lanthanide Cage	Angewandte Chemie International Edition	2025
34	臧双全、韩振	Stimuli-Responsive Circularly Polarized Luminescence of Gold Clusters Based on Hydrogen-Bond Driven Intercluster Coupling	Angewandte Chemie International Edition	2025
35	臧双全、黄仁武	Selectivity Modulation of Multistep Reduction Reactions by Gold Nanoclusters	Angewandte Chemie International Edition	2025
36	臧双全、李恺	Temperature-Inert Coinage Metal Cluster Scintillator	Angewandte Chemie International Edition	2025
37	臧双全、李恺	Short Lifetime Radical Metal Cluster Scintillator	Angewandte Chemie International Edition	2025

38	臧双全、李恺	Afterglow Copper(I) Iodine Cluster Scintillator	Angewandte Chemie International Edition	2025
39	臧双全、彭鹏	Pyrolysis-Free Synthesis of Synergistic Single-Atom/Nanocluster Electrocatalysts for Hydrogen Evolution	Angewandte Chemie International Edition	2025
40	臧双全、王朝阳	All-Nido-Carborane-Protected Copper Clusters	Angewandte Chemie International Edition	2025
41	臧双全、王锐	3D Cluster-Based Covalent Organic Framework for Efficient CO2 Photoreduction	Angewandte Chemie International Edition	2025
42	臧双全、杨圆	An Atomically Precise Copper Cluster Nanoreactor for Efficient Catalysis in Chemical Fixation of Low-Concentration CO2	Angewandte Chemie International Edition	2025
43	陈卫华	Anion-Tailored EDL Induced Triple-Layer SEI on High-Capacity Anodes Enabling Fast-Charging and Durable Sodium-Storage	Angewandte Chemie-International Edition	2025
44	李保军	MXene-Supported Ru–Ni: A Common Active Site for Hydrolysis, Hydrogen Oxidation, and Hydrogenation	Angewandte Chemie-International Edition	2025
45	刘清朝	Harnessing 4f Electron Itinerancy for Integrated Dual-Band Redox Systems Boosts Lithium-Oxygen Batteries Electrocatalysis	Angewandte Chemie-International Edition	2025

46	刘清朝	Electron Itinerancy Mediated by Oxygen Vacancies Breaks the Inert Electron Chain to Boost Lithium–Oxygen Batteries Electrocatalysis	Angewandte Chemie-International Edition	2025
47	赵英杰（通讯作者）	Marangoni Flow Reinforced Stencil Printing of Perovskite Single‐Crystal Arrays Toward Functional Optoelectronic Devices.	Angewandte Chemie-International Edition	2025
48	郭玮	The Key of Zn2+ Transfer Kinetics in Zinc Metal Batteries	Chem	2025
49	牛林彬	Manganese low-energy photocatalysis for remodeling nitrogenation of alkenes	Chem	2025
50	陈卫华	Unveiling gas production in rechargeable batteries via insitu differential electrochemical masss pectrometry	Chemical Society Reviews	2025
51	付永柱	Ligand Exchange of Li-ion Solvation Sheath Enables Balanced Electrolytes	Joule	2025
52	张懿强、李鹏伟	Achieving low-n value phases and unobstructed carrier transport toward high-performance quasi-2D perovskite solar cells and modules	Joule	2025
53	陈学年	A Borenium-Borane Composite for Exhaustive Reduction of Oxo-Chemicals	Journal of the American Chemical Society	2025
54	邓瑞显	Taming Enolate Regioselectivity: Catalyst-Guided Divergent Synthesis of Atropisomeric Pyridones via Switchable C- and O-Acylation	Journal of the American Chemical Society	2025

55	郭玮	Molecular Evolution of Target Organosulfur Enables High-performance Aqueous Zinc Batteries	Journal of the American Chemical Society	2025
56	郭玮	Dissolution Inhibition via Intramolecular N···I Halogen Bond Enables High-loading Zn-organic Battery	Journal of the American Chemical Society	2025
57	郭玮	Aqueous Zinc−Organoiodine Battery with High Kinetics and Dense Cathodes	Journal of the American Chemical Society	2025
58	侯红卫	Giant Enhancement of Optical Nonlinearity by Manipulating Guest Molecular Stacking Modes in Metal−Organic Frameworks	Journal of the American Chemical Society	2025
59	李占伟	Unveiling the Synergistic and Perforation-Dominant Self-Assembly Mechanisms of Supramolecular Chiral Helical Microtoroids	Journal of the American Chemical Society	2025
60	唐帅和付永柱	Topological Design of Highly Conductive Weakly Solvating Electrolytes for Ultrastable Sodium Metal Batteries Operating at −60°C and Below	Journal of the American Chemical Society	2025
61	王伟	A Hexavalent Tellurium-Based Chalcogen Bonding Catalysis Platform: High Catalytic Activity and Controlling of Selectivity	Journal of the American Chemical Society	2025
62	臧双全	Atomically Precise Copper Cluster for Highly Chemoselective Carbenoid Insertion into the N–H Bond of Aliphatic Amine	Journal of the American Chemical Society	2025
63	臧双全	Ultrastable Copper Cluster Enables Highly Site-Selective and Chemoselective Carbocation C(sp3)–H and C(sp2)–H Bonds Functionalization	Journal of the American Chemical Society	2025

64	臧双全	Visualization of Total Synthesis from Au11 to Au13 Nanoclusters	Journal of the American Chemical Society	2025
65	臧双全	Macroscopic Gold Cluster Helical Tendrils	Journal of the American Chemical Society	2025
66	臧双全	Consecutive C–C Coupling of CH4 and CO2 Mediated by Heteronuclear Metal Cations CuTa+	Journal of the American Chemical Society	2025
67	臧双全、陈高松	Pressure-Activated Efficient Near-Infrared Luminescence in Atomically Precise Gold Nanoclusters	Journal of the American Chemical Society	2025
68	臧双全、陈高松	Pressure-Driven Circularly Polarized Luminescence Enhancement and Chirality Amplification	Journal of the American Chemical Society	2025
69	臧双全、孙国强、刘晓飞	High-Performance Hypergolic Fuels Based on Copper Hydride Clusters	Journal of the American Chemical Society	2025
70	臧双全、王朝阳	Atomic-Precise Active Site Surgery on Carboranylthiolate-Protected Silver Nanocluster Catalysts	Journal of the American Chemical Society	2025
71	陈卫华	Precisely Deciphering Solid Electrolyte Interphase	Matter	2025
72	李鹏伟	Machine learning-driven ligand engineering decodes and controls structural distortions in 2D perovskites	Matter	2025

73	卢思宇	Carbon-based nanomaterials for carbon neutralization through electrochemical CO2 reduction and C–N coupling	Matter	2025
74	潘琪	Recent advances in multidimensional micro/nano structures for optoelectronic devices: Structures, properties, and performance	Matter	2025
75	臧双全、蔡金孟	Chiral-induced spin selectivity in electrocatalysis	Matter	2025
76	李二庆	Newly developed Pd/ZU-Phos/DBN cooperative catalysis enables enantioselective [4 + 2] annulations for efficient synthesis of diverse spirocyclic scaffolds	National Science Review	2025
77	卢思宇	Current status and future prospects of non-toxicity carbon-dot-based miniaturized lasers	National Science Review	2025
78	卢思宇	Current status and future prospects of non-toxicity carbon-dot-based miniaturized lasers	National Science Review	2025
79	孟红敏（一作）	Ane pH-driven DNA nanodevice for impeding metastasis in vivo by selectively blocking cell signaling	National Science Review	2025
80	臧双全、蔡金孟	Atomically precise silver-based bimetallic clusters for electrocatalytic urea synthesis	National Science Review	2025
81	臧双全、李恺	Thermally activated delayed phosphorescence triggered by charge	National Science Review	2025

		separation state carrier storage in an organic scintillator		
82	贾师琦	Organocatalytic enantioselective synthesis of double S-shaped quadruple helicene-like molecules	Nature Communication	2025
83	臧双全	Solvent-mediated chirality inversion in orthogonal hierarchical assembly of achiral carbene-anchored gold cluster	Nature Communication	2025
84	臧双全	Self-assembled metal clustersomes and chirality transfer to colloidal photonic crystals	Nature Communication	2025
85	臧双全	Tightly bonded excitons in chiral metal clusters for luminescent brilliance	Nature Communication	2025
86	臧双全、韩振	Maximized circularly polarized luminescence from metal clusters accelerates chiral photopolymerization	Nature Communication	2025
87	臧双全、李海洋	Photo-controlled vacancies and conductivity within single crystals of silver chalcogenolate cluster-based MOFs	Nature Communication	2025
88	臧双全、袁迎雪	Chiral metal cluster-mediated chirality transfer in light-harvesting nanoribbons for amplified circularly polarized luminescence	Nature Communication	2025
89	常江伟	Engineering high-density microcrystalline boundary with V-doped RuO2 for high-performance oxygen evolution in acid	Nature Communications	2025
90	陈卫华	Locking-chain electrolyte additive enabling moisture-tolerant electrolytes for sodium-ion batteries	Nature Communications	2025

91	卢思宇	Engineering high-density microcrystalline boundary with V-doped RuO2 for highperformance oxygen evolution in acid	Nature Communications	2025
92	梅光建	Organocatalytic asymmetric synthesis of Tröger’s bases	Nature Communications	2025
93	魏东辉	An analysis method including orbital overlap directions for predicting π electron properties and reactivity vectors	Nature Communications	2025
94	赵英杰（第一作者）	Direct photo-patterning of halide perovskites toward machine learning-assisted erasable photonic cryptography	Nature Communications	2025
95	贾师琦	Chiral medium-sized rings beyond central chirality	Nature Reviews Chemistry	2025
96	臧双全、陈高松	Unprecedented stacking-dependent piezoluminescence enhancement in atomically precise superatomic gold nanoclusters	Science Advances	2025
97	臧双全、袁迎雪	Gold clusters assembled homochiral helical microbowties	Science Advances	2025
98	张田原；郝新奇	Electrochemical C4 alkylation of pyridine derivatives: Enhanced regioselectivity via silane assistance	Science Advances	2025

	2024 年 高 水 平 论 文			
序号	通讯作者	论 文 题 目	期 刊	出版时间
1	臧双全、董喜燕	Chemical Flexibility of Atomically Precise Metal Clusters	Chem. Rev.	2024
2	臧双全、李恺	Chiral silver cluster-based light-harvesting systems: Enantioselective chirality transfer and amplified circularly polarized luminescence	Chem	2024
3	臧双全、王朝阳	Stepwise structural evolution toward robust carboranealkynyl- protected copper nanocluster catalysts for nitrate electroreduction	Sci. Adv.	2024
4	臧双全、黄仁武	Atomically precise copper clusters with dual sites for highly chemoselective and efficient hydroboration	Nat. Commun.	2024
5	臧双全、罗曦明	Hierarchical assembly of Ag40 nanowheel ranging from building blocks to diverse superstructure regulation	Nat. Commun.	2024
6	臧双全	Single-atom tailored atomically-precise nanoclusters for enhanced electrochemical reduction of CO2-to-CO activity	Nat. Commun.	2024
7	臧双全	Filling the gaps in icosahedral superatomic metal clusters	Natl Sci Rev	2024

8	臧双全、董喜燕	Carborane-Cluster-Wrapped Copper Cluster with Cyclodextrin-like Cavities for Chiral Recognition	J. Am. Chem. Soc.	2024
9	臧双全、王朝阳	Thiacalix[4]arene Etching of an Anisotropic Cu70H22 Intermediate for Accessing Robust Modularly Assembled Copper Nanoclusters	J. Am. Chem. Soc.	2024
10	臧双全、王锐、赵淑娜	Promoting CO2 Electroreduction to Hydrocarbon Products via Sulfur-Enhanced Proton Feeding in Atomically Precise Thiolate-Protected Cu Clusters	Angew. Chem. Int. Ed.	2024
11	臧双全、韩振	Reversible Local Protonation-Deprotonation: Tuning Stimuli-Responsive Circularly Polarized Luminescence in Chiral Hybrid Zinc Halides for Anti-Counterfeiting and Encryption	Angew. Chem. Int. Ed.	2024
12	臧双全	Atomically Precise Chiral Metal Nanoclusters for Circularly Polarized Light Detection	Angew. Chem. Int. Ed.	2024
13	臧双全、陈高松	Vibration-Dependent Dual-Phosphorescent Cu4 Nanocluster with Remarkable Piezochromic Behavior	Angew. Chem. Int. Ed.	2024
14	臧双全	Microwave-Assisted Rapid Synthesis of MOF-Based Single-Atom Ni Catalyst for CO2 Electroreduction at Ampere-Level Current	Angew. Chem. Int. Ed.	2024
15	臧双全、蔡金孟	Tandem Nitrate-to-Ammonia Conversion on Atomically Precise Silver Nanocluster/MXene Electrocatalyst	Angew. Chem. Int. Ed.	2024
16	臧双全、黄仁武、蔡金孟	Electrocatalytic Nitrate Reduction on Metallic CoNi-Terminated Catalyst with Industrial-Level Current Density in Neutral Medium	Adv. Mater.	2024
17	付永柱	An Ultrastable Low-temperature Na Metal Battery Enabled by Synergy between Weakly Solvating Solvents	J. Am. Chem. Soc.	2024

18	郭玮	From Inorganic to Organic Iodine: Stabilization of I+ Enabling High-Energy Lithium-Iodine Battery	J. Am. Chem. Soc.	2024
19	付永柱	Facilitating Ultra-Stable O3-type Cathode for 4.5 V Sodium-ion Batteries via Dual-Reductive Coupling Mechanism	J. Am. Chem. Soc.	2024
20	付永柱	Highly Reversible Transition Metal Migration in Superstructure-free Li-rich Oxide Boosting Voltage Stability and Redox Symmetry	Nat. Commun.	2024
21	王鑫	When chiral chemistry meets electrochemistry: A virgin land of an academic gold mine	Matter	2024
22	蓝宇、李世俊、牛林彬	Iron photocatalysis via Brønsted acid-unlocked ligand-to-metal charge transfer	Nat. Commun.	2024
23	贾师琦,牛林彬,蓝宇	Strategies and Mechanisms of First-Row Transition Metal-Regulated Radical C–H Functionalization	Chem. Rev.	2024
24	蓝宇、李世俊、牛林彬	Heterocoupling Two Similar Benzyl Radicals by Dual Photoredox/Cobalt Catalysis	Angew. Chem. Int. Ed.	2024
25	卢思宇	Synthesis of ultrahigh-metal-density single-atom catalysts via metal sulfide-mediated atomic trapping	Nature Synthesis	2024
26	卢思宇	Atomically engineered interfaces inducing bridging oxygen-mediated deprotonation for enhanced oxygen evolution in acidic conditions	Nat. Commun.	2024
27	卢思宇	A Robust Anti-Thermal-Quenching Phosphor Based on Zero-Dimensional Metal Halide Rb3InCl6: x Sb3+	J. Am. Chem. Soc.	2024

28	卢思宇	Oxygen Radical Coupling on Short-Range Ordered Ru Atom Arrays Enables Exceptional Activity and Stability for Acidic Water Oxidation	J. Am. Chem. Soc.	2024
29	卢思宇	Hydrogen Bond-Induced Flexible and Twisted Self-Assembly of Functionalized Carbon Dots with Customized-Color Circularly Polarized Luminescence	Angew. Chem. Int. Ed.	2024
30	卢思宇	Concentration-Switchable Assembly of Carbon Dots for Circularly Polarized Luminescent Amplification in Chiral Logic Gates and Deep-Red Light-Emitting Diodes	Adv. Mater.	2024
31	卢思宇	Tailored Fabrication of Full-Color Ultrastable Room-Temperature Phosphorescence Carbon Dots Composites with Unexpected Thermally Activated Delayed Fluorescence	Adv. Mater.	2024
32	卢思宇	Lasing of carbon dots: Chemical design, mechanisms, and bright future	Chem	2024
33	卢思宇	Unveiling the photoluminescence mechanisms of carbon dots through tunable near-infrared dual-wavelength lasing	Matter	2024
34	卢思宇	Advances in shell and core engineering of carbonized polymer dots for enhanced applications	Accounts of Chemical Research	2024
35	卢思宇	Cl^{-}-repelling CoFe-LDH enables ultrastable and ampere-level seawater electrocatalysis	Matter	2024
36	陈卫华	Edge Electron Effect Induced High-Entropy SEI for Durable Anode-Free Sodium Batteries	Adv. Mater.	2024
37	陈卫华	Anion-Tailored EDL Induced Triple-Layer SEI on High-Capacity Anodes Enabling Fast-Charging and Durable Sodium-Storage	Angew. Chem. Int. Ed.	2024

38	陈卫华	Interface-Compatible Gel-Polymer Electrolyte Enabled by NaF Solubility-Regulation toward All-Climate Solid-State Sodium Batteries	Angew. Chem. Int. Ed.	2024
39	陈晓岚	Energy-Transfer-Enabled Photocatalytic Transformations of Aryl Thianthrenium Salts	Nat. Commun.	2024
40	陈学年	Facile Synthesis of Potassium Decahydrido-Monocarba-closo-Decaborate Imidazole Complex Electrolyte for All-Solid-State Potassium Metal Batteries	Angew. Chem. Int. Ed.	2024
41	崔秀灵	Enantioselective de novo construction of 3-oxindoles via organocatalyzed formal [3+2] annulation from simple arylamines	Nat. Commun.	2024
42	邓瑞显、石林林	Regio- and Atroposelective Ring-Opening of 1H-Benzo[4,5]oxazolopyridinones	Angew. Chem. Int. Ed.	2024
43	邓瑞显	Symmetric Anion Mediated Dynamic Kinetic Asymmetric Knoevenagel Reaction for NC and NN Atropisomers Synthesis	Angew. Chem. Int. Ed.	2024
44	李丹，郭再萍	Olivine-Type Fe2GeX4 (X = S, Se, and Te): A Novel Class of Anode Materials for Exceptional Sodium Storage Performance	Adv. Mater.	2024
45	李宏基	Photothermal catalytic transfer hydrogenolysis of protolignin	Nat. Commun.	2024
46	李铁生	Upconversion/Downshifting Circularly Polarized Luminescence over 1200 nm in a Single Nanoparticle for Optical Anticounterfeiting and Information Encryption	Angew. Chem. Int. Ed	2024
47	李禹函	Asynchronous Ring Opening of Cyclic Carbonate and Glycidyl Ether Induced Phase Evolution Towards Heat-free and Rapid-bonding Superior Epoxy Adhesive	Angew. Chem. Int. Ed.	2024

48	刘清朝	Harnessing 4f Electron Itinerancy for Integrated Dual-Band Redox Systems Boosts Lithium-Oxygen Batteries Electrocatalysis	Angew. Chem. Int. Ed.	2024
49	吕超	Aggregation-induced emission-active supramolecular polymers: from controlled preparation to applications	Chem. Soc. Rev.	2024
50	马艳娜	B(9)-OH-o-Carboranes: Synthesis, Mechanism, and Property Exploration	J. Am. Chem. Soc.	2024
51	梅光建	Catalytic asymmetric synthesis of planar-chiral dianthranilides via (Dynamic) kinetic resolution	Nat. Commun.	2024
52	梅光建	Azocarboxamide-enabled enantioselective regiodivergent unsymmetrical 1,2-diaminations.	Nat. Commun.	2024
53	梅光建	A Chemically Powered Rotary Molecular Motor Based on Reversible Oxazepine Formation	Angew. Chem. Int. Ed.	2024
54	孙晨凯、张懿强、宋延林	Unveiling the Potential ofTwo-Terminal Perovskite/Organic Tandem Solar Cells: Mechanisms, Status, and Challenges	Adv. Mater.	2024
55	吴俊良	Regio- and stereoselective access to highly substituted vinylphosphine oxides via metalfree electrophilic phosphonoiodination of alkynes	Nat. Commun.	2024
56	杨波	Bioinspired Self-Assembly of Metalloporphyrins and Polyelectrolytes into Hierarchical Supramolecular Nanostructures for Enhanced Photocatalytic H2 Production in Water	Angew. Chem. Int. Ed.	2024
57	杨丹丹、牛俊龙	Simultaneous construction of inherent and axial chirality by cobalt-catalyzed enantioselective C-H activation of calix[4]arenes	Nat. Commun.	2024

58	余斌，常俊标	2′-Fluorinated Nucleoside Chemistry for New Drug Discovery: Achievements and Prospects	National Science Review	2024
59	张懿强	Governing the dispersion of quasi-2D perovskite phases toward efficient and stable perovskite solar cells	Matter	2024
60	张懿强	Additive-Driven Enhancement of Crystallization: Strategies and Prospects for Boosting Photoluminescence Quantum Yields in Halide Perovskite Films for Light-Emitting Diodes	Adv. Mater.	2024
61	张懿强	Lead-Chelating Intermediate for Air-Processed Phase-Pure FAPbI3 Perovskite Solar Cells	Angew. Chem. Int. Ed.	2024